

Purdue University

Purdue e-Pubs

---

International Refrigeration and Air Conditioning  
Conference

School of Mechanical Engineering

---

2021

## Bubble Dynamics Studies In An Absorber With Swirl Entry Of Absorption Refrigeration System

Narasimha Reddy Sanikommu

*Indian Institute of Technology Madras, India, mania@iitm.ac.in*

Mani Annamalai

*Indian Institute of Technology Madras, India*

Tiwari Shaligram

Follow this and additional works at: <https://docs.lib.purdue.edu/iracc>

---

Sanikommu, Narasimha Reddy; Annamalai, Mani; and Shaligram, Tiwari, "Bubble Dynamics Studies In An Absorber With Swirl Entry Of Absorption Refrigeration System" (2021). *International Refrigeration and Air Conditioning Conference*. Paper 2140.

<https://docs.lib.purdue.edu/iracc/2140>

This document has been made available through Purdue e-Pubs, a service of the Purdue University Libraries.

Please contact [epubs@purdue.edu](mailto:epubs@purdue.edu) for additional information.

Complete proceedings may be acquired in print and on CD-ROM directly from the Ray W. Herrick Laboratories at <https://engineering.purdue.edu/Herrick/Events/orderlit.html>

# Bubble dynamics studies in an absorber with swirl entry of an absorption refrigeration system

Narasimha Reddy Sanikommu, Mani A\*, Shaligram Tiwari

Refrigeration and Air Conditioning Laboratory, Department of Mechanical Engineering, Indian Institute of Technology Madras, Tamil Nadu, India.

\* Corresponding Author: Tel.:+91 44 22574666; fax: +91 44 22570509  
Email address: mania@iitm.ac.in

## ABSTRACT

Experimental investigations have been carried out on a glass bubble absorber with swirl entry of air to visualize air bubble characteristics. Experiments are carried out in still, co-current and counter-current flow direction of the water. In bubble visualization studies, it was observed that the bubbles form at the swirl generator surface, grow and detach from the swirl generator surface and move upwards in water. Effect of air and water flow rate on the bubble detachment diameter was studied. Bubble detachment diameter always increases with air flow rate irrespective of water flow direction. Bubble diameter increases in counter-current flow of water, whereas it decreases in co-current flow of water.

## 1. INTRODUCTION

Multiphase flows find its application in absorbers, distillation columns, and chemical processing plants, etc. In bubble absorber, the gas is injected into the liquid pool with the help of an orifice. Absorber in a Vapour Absorption Refrigeration System (VARS) is considered as one of the critical components due to lower heat and mass transfer coefficients associated with the absorption phenomenon (Castro *et al.*, 2009). Typically, falling film and bubble absorbers are used in most refrigeration applications due to their ability to effectively remove exothermic heat and high heat and mass transfer coefficients among the other configurations (Lee *et al.*, 2003; Castro *et al.*, 2009). In bubble absorber, the refrigerant vapour is bubbled through a weak solution by using a nozzle. Refrigerant vapour bubble will grow from the nozzle, detach and rise upwards through a solution, resulting in an increase in interfacial area between vapour and solution than that of falling film absorber. Generation of flow with spiral motion in a tangential direction in addition to axial and radial directions is termed as swirling flow. Swirling flow can be produced with the help of a swirl generator, which is considered as a passive heat transfer enhancement technique. Swirl flows can be classified into three types depending on the velocity profile characteristics: continuous swirl flow, rotation, and decaying swirl flow (Razgaitis and Holman, 1976). In the present study, swirl flow is produced by the decaying type swirl generator.

Design and the performance characteristics of bubble absorber mainly depend on the bubble hydrodynamic characteristics (Akita and Yoshida, 1974). Authors had carried out the experimental studies to estimate the interfacial area, bubble size distribution, etc. using a photographic method with air-water, oxygen-water, air-glycol, air-methanol and aqueous sodium sulphate solutions as working fluids. They reported that the mass transfer coefficient was increased mainly due to the smaller bubble size, which resulted in increased interfacial area. Also, the initial bubble diameter was dependent only on orifice diameter and gas velocity. Effect of liquid viscosity on bubble diameter and overall mass transfer coefficient was studied by Bhavaraju *et al.* (1978). The results manifested that the high interfacial area and intense liquid mixing was achieved with low viscosity liquids. Gaddis and Vogelpohl (1986) developed a theoretical correlation of bubble detachment diameter in quiescent liquid under constant gas flow conditions. Bubble size correlation was developed by Bhunia *et al.* (1998) for co-flowing liquid conditions under normal and reduced gravity conditions. Authors reported that the bubbles were of more size and more spherical under reduced gravity conditions until 0.01 g. Bai and Thomas (2001) experimentally and

numerically studied the effect of downward liquid flow on horizontally injected gas bubble evolution and its characteristics.

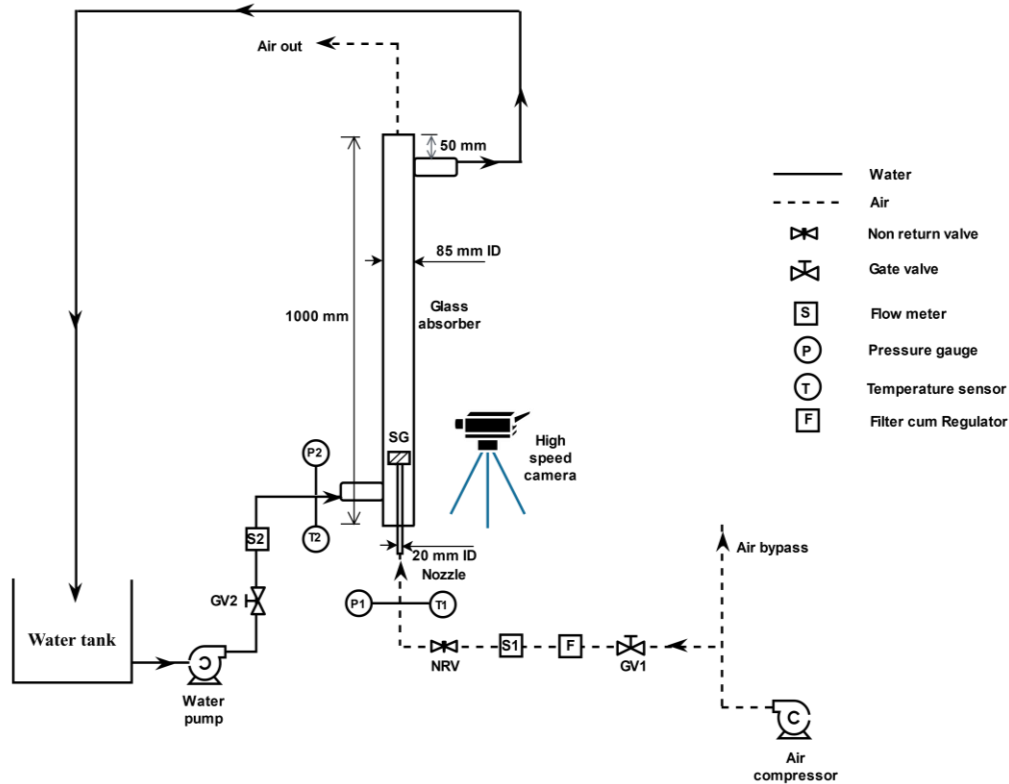
Bubble behaviour in an ammonia-water VARS was visualized by Tae *et al.* (2002). The orifice diameter, number of orifices, solution concentration and gas velocities were the key parameters influencing the bubble size. Authors observed that the departing bubbles were hemispherical for inertial force dominant flow, whereas bubbles were spherical for surface tension dominant flow. The bubble breakup was faster in the co-flowing fluid than in quiescent liquid, hence creating a smaller bubble size in co-flowing fluid conditions (Chakraborty *et al.*, 2011). Quasi-static bubble growth from a submerged nozzle in water was investigated experimentally by high-speed photography and concluded that the smallest orifice resulted in smaller bubbles, less departing time and more spherical shape (Bari and Robinson, 2013). Suresh and Mani (2012) carried out experimental investigations on glass bubble absorber in VARS working with R134a-DMF to visualize the bubble behaviour and study the effect of gas flow rate on absorption rate. Based on the experimental results, the authors developed a correlation for bubble diameter during detachment. Panda and Mani (2014) carried out visualization studies to understand the characteristics of the tangential entry of air bubbles in different water flow directions with multiple nozzles and nozzle angles. Results had shown that there was no variation in bubble diameter with multiple numbers of nozzles and single nozzle. Also, the bubble diameter was increased with an increase in nozzle angle.

To increase the bubble absorber performance further and to alleviate the poor heat and mass transfer coefficients associated with the absorber, the present study introduces a passive enhancement technique. Since the bubbles hydrodynamic characteristics influence the heat and mass transfer characteristics in the absorber, the present study focuses on experimental investigations to visualize the bubble behaviour with swirl entry of air in still and flowing water situations. Effect of the air and water flow rates on bubble diameter during detachment is studied.

## 2. EXPERIMENTAL SETUP

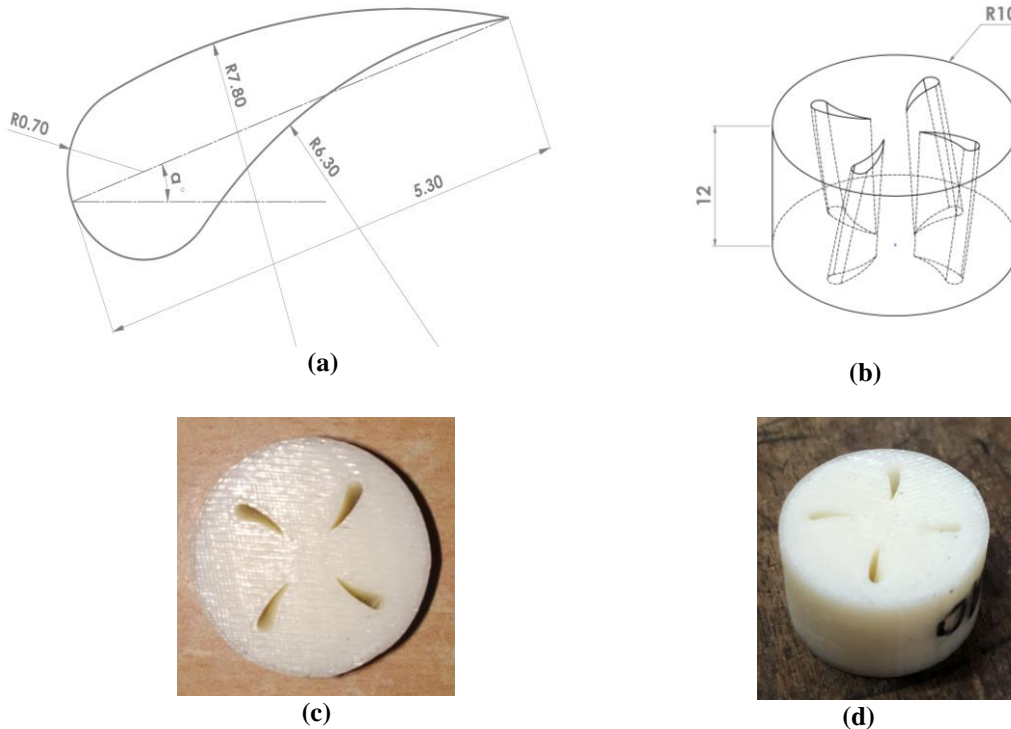
Visualization experiments have been carried out to observe the bubble characteristics in swirl entry of air in a vertical glass tube test section, as shown in Figure 1. The experimental setup consists of a glass bubble absorber (1000 mm length, 85 mm ID and 89 mm OD), water tank, water pump, air compressor, swirl generator, pressure, temperature and flow measuring instruments, and valves. Air is supplied from a two-stage reciprocating compressor (maximum working pressure of 12.5 bar and storage tank capacity of 220 litres) through an air filter cum regulator, air rotameter and injected through a swirl generator (SG) installed at the bottom of the glass tube. The swirl generator geometry and its dimensions are shown in Figure 2. The cavity type of swirl decay generator is modelled based on the proposed profile geometry in Figure 2. Number of nozzles ( $N$ ) and profile geometry is chosen by carrying out the single-phase numerical simulations with air in which both camber angle ( $0^\circ$ ,  $10^\circ$  and  $20^\circ$ ) and twist angle ( $0^\circ$ ,  $10^\circ$  and  $20^\circ$ ) were varied. Camber angle ( $\alpha$ ) is defined as the angle between the radial line passing through stagnation of the leading edge and the chord. Angle between the line passing through the leading edge and longitudinal cylinder edge is defined as a twist or sweep angle ( $\theta$ ). The numerical simulation results had shown that the geometry with zero camber angle and  $20^\circ$  twist angle with four number of nozzles shown a better performance than the other generated profiles and number of nozzles (2, 3, 4 and 5). Then, the swirl generator is fabricated with the help of 3D printing.

All the experiments are carried out under constant air inlet pressure of 1.2-1.5 bar, which is achieved by bypassing some amount of air from the compressor tank. A non-return valve is fixed in the airline to avoid the backflow of water in the absence of air supply. A multi-stage centrifugal pump (capacity of  $1.5 \text{ m}^3/\text{hr}$  with a differential head of 20 m) is used to supply water either counter-current or co-current directions of water concerning airflow direction. The water outlet from a glass tube is connected back to the tank and air in these cases will escape from the absorber's top opening into the atmosphere. Bypass valve, control valve, and rotameter are used to control the water flow rate in the water circuit. All the measuring instruments are pre-calibrated. A high-speed camera with frame rates ranging from 350 fps to 600 fps is placed near the glass absorber to capture the bubble images near the swirl generator. The rotameter used to measure the water flow rate is having a measurement uncertainty of  $\pm 4\%$ . Air rotameter has an uncertainty of 2% in flow measurement. Pressure gauges having an uncertainty of  $\pm 1\%$  and copper-constant thermocouples having an uncertainty of  $\pm 0.5^\circ\text{C}$  are used.



**Figure 1:** Schematic diagram of the experimental setup

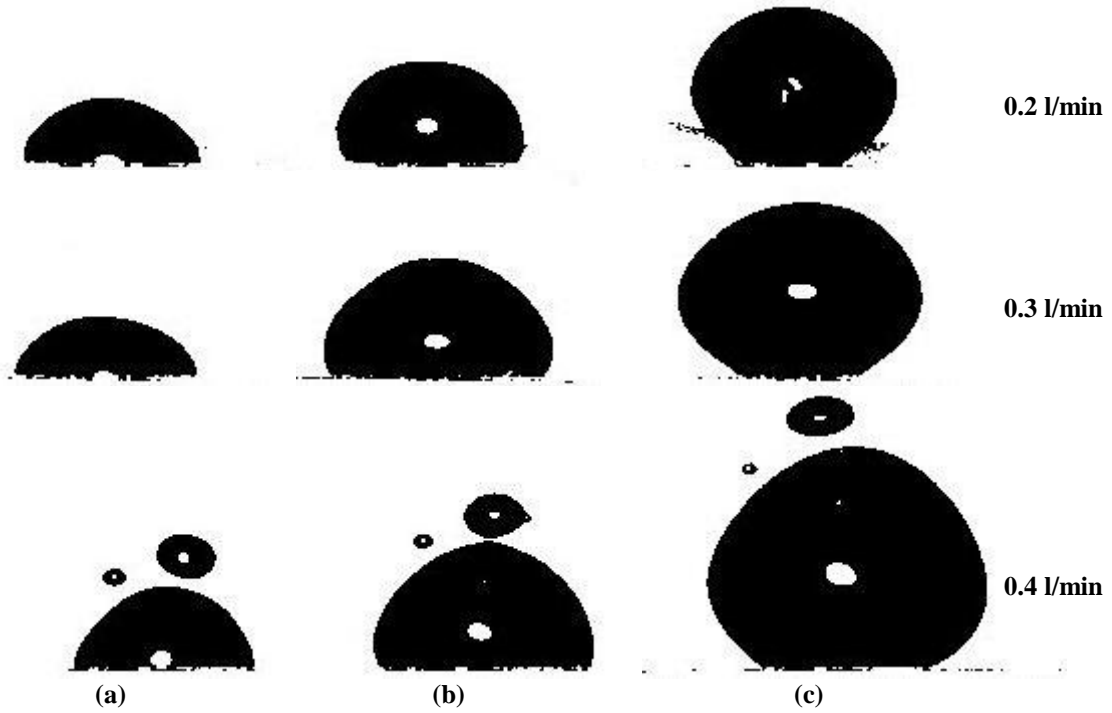
Initially, the compressor is switched on, and the discharge valve is kept closed for pressure building in storage tank up to 3bar. Bypass valve and flow control valve is then opened to allow the airflow through the separator cum regulator, rotameter, non-return valve, and swirl generator to glass absorber. The air pressure at the inlet of the absorber is always maintained at 1.2-1.5 bar with the help of air separator cum controller. Then, the centrifugal pump is turned on to supply water at desired flow rate and flow configuration can be maintained by altering water direction. Airflow is always started before the water flow to avoid the backflow of water into the air circuit. Desired air flow rate and water flow rate is maintained, and photographs are taken using a high-speed camera to capture the bubbles in growing and detachment stages. These bubble photographs are taken along with the referenced object placed inside a bubble absorber. The photographs are analyzed with the open source image processing software to calculate the bubble diameter during detachment. Initially, a reference object is calibrated with open source image processing software, and the uncertainty of  $\pm 5\%$  is found with the repeated measurements. The errors in measurement are due to distortion and location of bubble surfaces. Image processing techniques like colour balance, brightness and threshold are used to improve the quality of images to account for accurate measurements. The uploaded 2D bubble photographs in open source image processing software are observed to be either spherical or hemispherical or elliptical, and it is divided into a number of segments to calculate the radius.



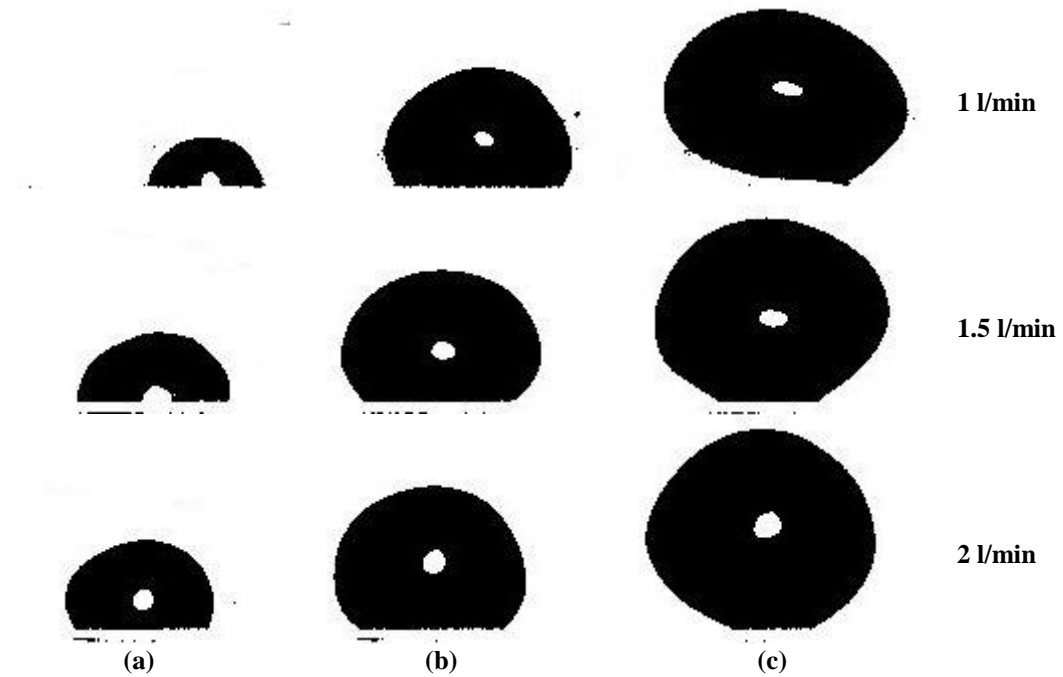
**Figure 2:** (a) Swirl generator profile geometry (all dimensions are in mm); (b) Swirl generator model; (c) 3D printed swirl generator top view and (d) 3D printed swirl generator

### 3. RESULTS AND DISCUSSION

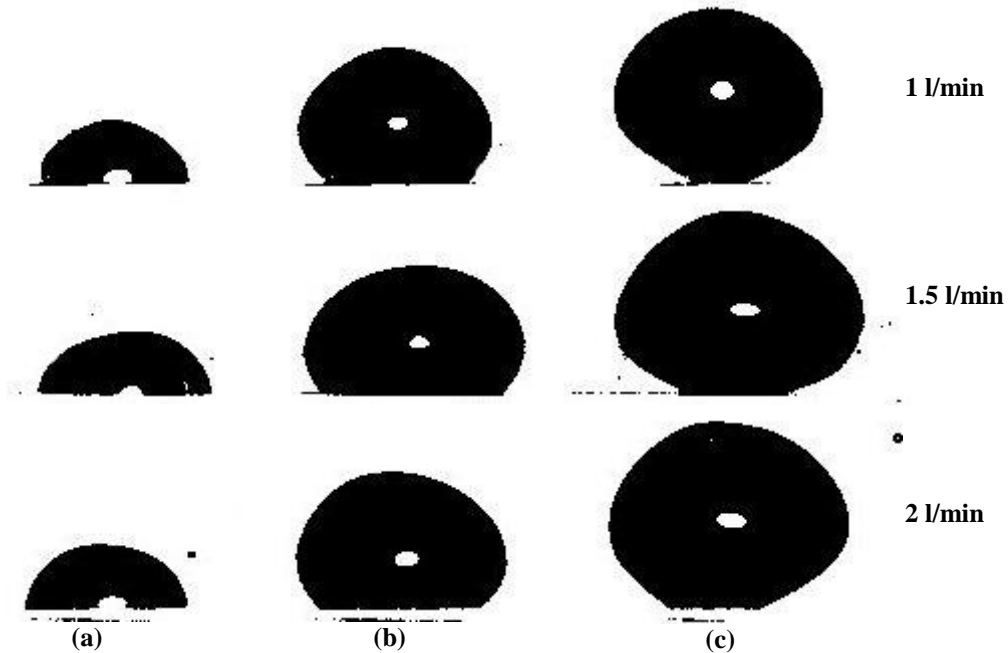
Experiments are conducted in glass bubble absorber by varying the operating parameters viz. air flow rate ( $Q_{\text{air}}$ ) ranging from 0.2 l/min to 0.7 l/min and water flow rates ( $Q_{\text{water}}$ ) from 1 l/min to 3.5 l/min. Water temperature is maintained at room temperature and pressure at slightly above the atmospheric. Figure 3 shows the photographs of air bubble formation at various stages in still water. From visualization of the photographs, the bubble evolution process can be divided into three stages based on its volume, namely: bubble formation, growth and detachment. In the bubble formation stage, the initiation of the bubble from swirl generator surface will take place based on the airflow rate. As the air is continually entering into bubble through swirl generator, the bubble volume increases and termed as bubble growth. In the detachment stage, the buoyancy force acting on bubble increases due to increased volume, hence the bubble leaves the swirl generator surface and move upwards through the water. Figures 4 and 5 show the visualization of air bubble formation at various stages in co-current, and counter-current water flows directions at 0.2 l/min air flow rate.



**Figure 3:** Visualization of air bubbles in still water at various airflow rates ((a) Bubble formation (b) Bubble growth (c) Bubble detachment)



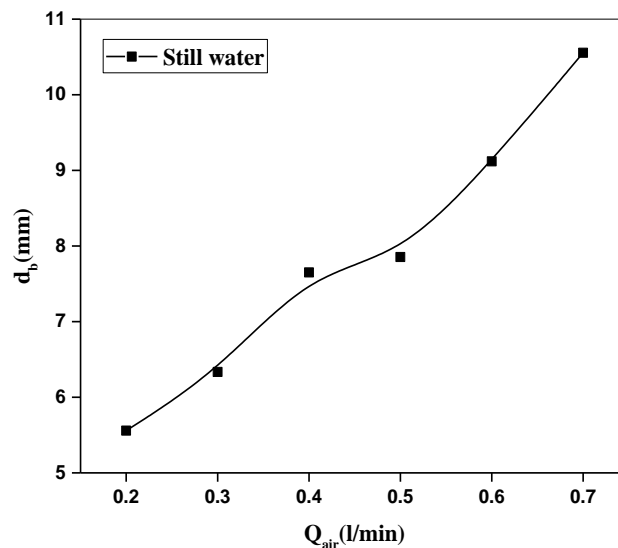
**Figure 4:** Visualization of air bubbles in a counter-current flow direction of water at 0.2 l/min air flow rate ((a) Bubble formation (b) Bubble growth (c) Bubble detachment)



**Figure 5:** Visualization of air bubbles in a co-current flow direction of water at 0.2 l/min air flow rate ((a) Bubble formation (b) Bubble growth (c) Bubble detachment)

### 3.1 Effect of airflow rate and water flow rate on bubble detachment diameter

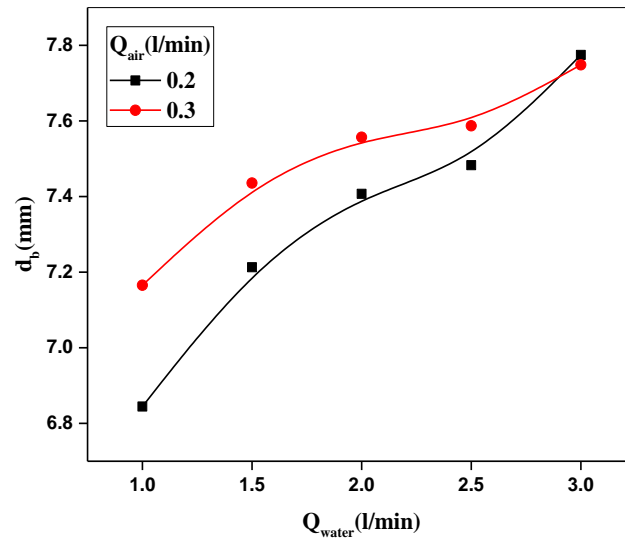
Figure 6 shows the variation of bubble detachment diameter ( $d_b$ ) with airflow rate in still water condition. It can be observed that the bubble detachment diameter during detachment increases with airflow rate. Also, bubbles tend to be spherical and smaller in size for lower airflow rates. As the air flow rate increases through a swirl generator, the amount of air in bubble increases, which resulted in increased bubble diameter.



**Figure 6:** Bubble detachment diameter variation with airflow rate in still water

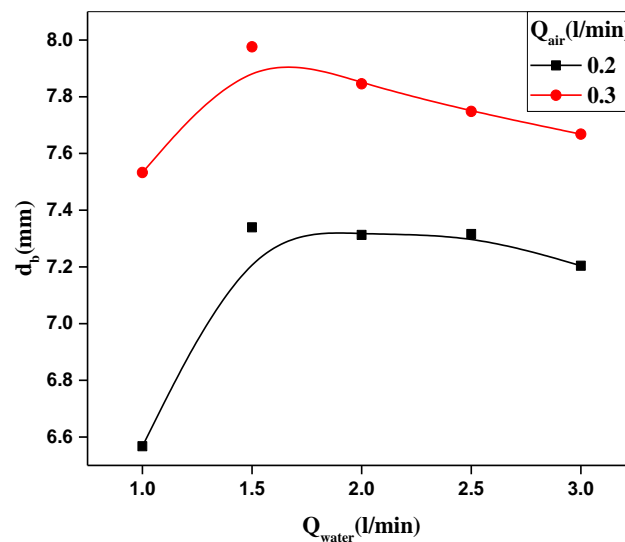
The detachment bubble diameter variation with a water flow rate in a counter-current water flow direction is shown in Figure 7. Results showed that the bubble diameter increases with an increase in water flow rate in the counter

flow. The counter flow of water exerts downward momentum on a growing bubble. Hence, the upward buoyancy force on the bubble is not enough to overcome the downward momentum force on the bubble, thus delaying the detachment and increasing bubble diameter.

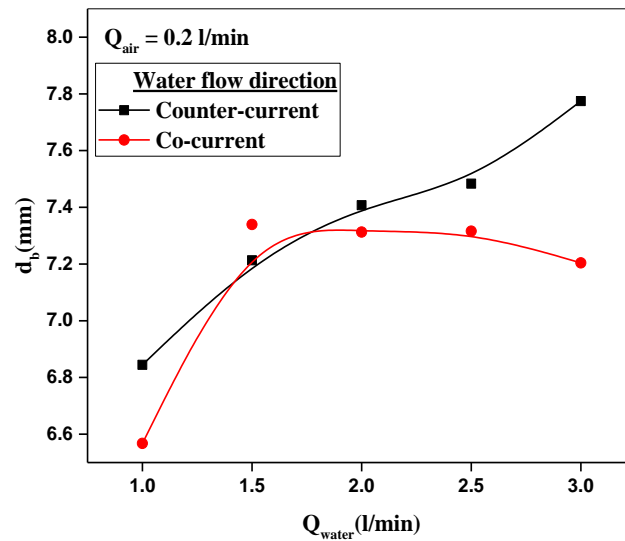


**Figure 7:** Bubble detachment diameter variation with a water flow rate in counter-current direction of water

Figure 8 shows the air bubble behaviour with water flow rate for co-current water conditions. Bubble diameter decreases with the increase in water flow rate. When the liquid is flowing upward, i.e. parallel to the airflow direction, water exerts a force on bubble surface in addition to the buoyancy force, which assists the bubble to detach early. As the water flow rate increases, the upward momentum imparted by water increases on bubble, which tends to detach earlier and resulted in small bubble diameter during detachment. It can also be seen that the increased bubble diameter with an increase in air flow rate. The bubble detachment diameter comparison for flowing conditions at 0.2 l/min of airflow rate is shown in Figure 9. It can be noticed that the co-current flow results in lower bubble diameter. It is attributed by the presence of assisting force to the bubble in co-current flow and opposing force to the bubble in counter-flow condition.





**Figure 8:** Bubble detachment diameter variation with water flow rate in the co-current direction of water**Figure 9:** Bubble detachment diameter comparison in flowing water condition

#### 4. CONCLUSIONS

Experimental investigations have been carried out on glass absorber to visualize the swirl entry of air bubble behaviour and to study the effect of air and water flow rates on the bubble detachment diameter. Bubble behaviour has been studied in still and flowing water conditions. The evolution process of bubbles is divided into bubble formation, growth and detachment stages. Bubble diameter during detachment increase with an increase in airflow rate in all conditions of water directions. In the counter flow direction of water, the bubble detachment diameter increases due to an increased downward momentum imparted by the counter current water on a bubble. The bubble detachment diameter decreases in co-current flow of water due to an increased upward momentum imparts by the co-current water along with buoyancy force.

#### NOMENCLATURE

ID	Inner diameter	(mm)
N	Number of nozzles	(-)
OD	Outer diameter	(mm)
R	Radius	(mm)
$Q_{\text{air}}$	Air flow rate	(l/min)
$Q_{\text{water}}$	Water flow rate	(l/min)
$D_b$	Bubble diameter	(mm)
$\alpha$	Camber angle	( $^{\circ}$ )
$\theta$	Twist angle	( $^{\circ}$ )
DMF	Dimethylformamide	
l/min	Liter per minute	
R134a	1,1,1,2-Tetrafluoroethane	
SG	Swirl Generator	
VARS	Vapour Absorption Refrigeration System	

## REFERENCES

- Akita, K. & Yoshida, F. (1974). Bubble Size, Interfacial Area, and Liquid-Phase Mass Transfer Coefficient in Bubble Columns. *Ind. Eng. Chem. Process Des. Dev.* 13, 84–91.
- Bai, H. & Thomas, B. G. (2001). Bubble formation during horizontal gas injection into downward-flowing liquid. *Metall. Mater. Trans. B Process Metall. Mater. Process. Sci.* 32, 1143–1159.
- Bari, S. di & Robinson, A. J. (2013). Experimental study of gas injected bubble growth from submerged orifices. *Exp. Therm. Fluid Sci.* 44, 124–137.
- Bhavaraju, S. M., Russell, T. W. F. & Blanch, H. W. (1978). The design of gas sparged devices for viscous liquid systems. *AIChE J.* 24, 454–466.
- Bhunia, A., Pais, S. C. & Kamotani, Y. (1998). Bubble Formation in a Coflow Configuration in Normal and Reduced Gravity. *AIChE J.* 44, 1499–1509.
- Castro, J., Oliet, C., Rodríguez, I. and Oliva, A. (2009). Comparison of the performance of falling film and bubble absorbers for air-cooled absorption systems. *Int. J. Therm. Sci.* 48, 1355–1366.
- Chakraborty, I., Biswas, G. & Ghoshdastidar, P. S. (2011). Bubble generation in quiescent and co-flowing liquids. *Int. J. Heat Mass Transf.* 54, 4673–4688.
- Gaddis, E. S. & Vogelpohl, A. (1986). Bubble formation in quiescent liquids under constant flow conditions. *Chem. Eng. Sci.* 41, 97–105.
- Lee, J.C., Lee, K.B., Chun, B.H., Lee, C.H., Ha, J.J. and Kim, S.H. (2003). A study on numerical simulations and experiments for mass transfer in bubble mode absorber of ammonia and water. *Int. J. Refrig.* 26, 551–558.
- Panda, S. K. & Mani, A. (2014). Experimental study on bubble absorber with multiple tangential nozzles. *15th Int. Refrig. Air Cond. Conf. Purdue* 1–10.
- Razgaitis, R., Holman, J.P. (1976). A survey of heat transfer in confined swirl flows. *Heat Mass Transfer Processes* 2, 831–866.
- Suresh, M. & Mani, A. (2012). Experimental studies on bubble characteristics for R134a-DMF bubble absorber. *Exp. Therm. Fluid Sci.* 39, 79–89.
- Tae, Y., Nagano, T. & Kashiwagi, T. (2002). Visualization of bubble behavior and bubble diameter correlation for NH<sub>3</sub>-H<sub>2</sub>O bubble absorption. *Int. J. Refrig.* 25, 127–135.